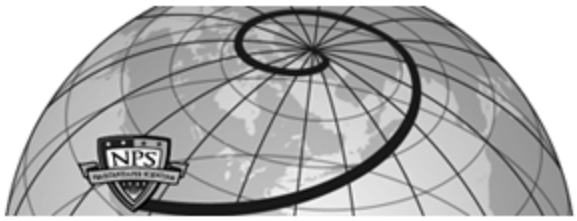

HELIX-PLASMA COUPLING

COLIN M. JONES

HELIX - PLASMA COUPLING

****

Colin M. Jones

HELIX - PLASMA COUPLING

by

Colin M. Jones
Lieutenant, United States Navy

Submitted in partial fulfillment of
the requirements for the degree of

MASTER OF SCIENCE
IN
ENGINEERING ELECTRONICS

United States Naval Postgraduate School
Monterey, California

1963

HELIX - PLASMA COUPLING

by

Colin M. Jones

This work is accepted as fulfilling
the thesis requirements for the degree of

MASTER OF SCIENCE

IN

ENGINEERING ELECTRONICS

from the

United States Naval Postgraduate School

ABSTRACT

As efforts continue to effectively utilize the microwave frequencies a need is apparent for a traveling wave type device capable of handling greater power at higher frequencies. One possible solution is the plasma microwave amplifier tube.

This paper discusses an analysis of the plasma - helix coupling problem which may hopefully lead to development of such a device whereby the R. F. energy is coupled directly to the plasma with a helix, rather than coupling to an electron beam as has been the case heretofore. A theoretical analysis is presented, and the computer solution to the analytical equations evolved and the resulting $\omega - \beta$ plots are included.

This writer wishes to express his appreciation for the assistance and inspiration provided by Dr. Glen A. Gray of the U. S. Naval Postgraduate School in carrying out this investigation.

TABLE OF CONTENTS

LIST OF ILLUSTRATIONS

1. Background.

The purpose of this investigation was to study the problem of coupling electromagnetic energy between a slow wave structure and a plasma column.

The underlying reason for interest in this problem is the design of a plasma microwave amplifier tube. A plasma microwave amplifier tube, where the plasma column acts as the slow wave structure, interacting with the electron beam, may well provide some advantages over present day types of traveling wave tubes. At the present time, conventional traveling wave tubes are limited in the power they can handle at high microwave frequencies. As frequency increases, it becomes difficult to construct a satisfactory slow wave structure which will dissipate any appreciable heat. Even at the lower microwave frequencies, heat dissipation in the slow wave structure may be a problem for high power applications. The plasma as a slow wave structure offers definite possibilities in that heat dissipation in the structure should no longer be a problem. There should be no inherent limitation insofar as mechanical dimensions are concerned, as the frequency is increased. Further, the plasma microwave amplifier device appears to offer promise of high gain and high power in a relatively small package.

The device proposed (Fig. (1)) is in many respects similar to a conventional traveling wave tube. The tube consists of a conventional

2

Fig. 1

electron gun assembly, a d.c. heated filament consisting of a .001" tungsten ribbon approximately 1/2" X 3/4" at either end of the interaction region, and two helix slow wave structures in the interaction region.

The concept is to generate a plasma by heating the two filaments to 2300^{o}C in a cesium gas environment at a very low pressure, on the order of 10^{-6} to 10^{-7} mm. Hg. These hot filaments will then cause contact ionization of the cesium gas thereby generating a plasma. R. F. energy is then coupled from the helix slow wave structure to the plasma, exciting the plasma. In turn, the electron beam on passing thru the plasma interacts with the wave excited on the plasma, giving a traveling wave type interaction.

A helix slow wave structure was chosen for several reasons. First, it is rather easily fabricated. Second, it has been used extensively in tube work, and experience is available regarding its characteristics. Finally, a theoretical analysis of the helix is available, Beck (1), and Hutter (2).

The cesium plasma was chosen for several reasons. First, the plasma frequency may be easily varied by control of the envelope temperature, and thereby the gas pressure. Second, it provides a relatively homogenous plasma, and may be quite highly ionized. Third, it provides a quiet plasma, that is, it is relatively free from spurious oscillations and noise. Finally, it may be readily ionized by contact

ionization. Since the ionization voltage of the cesium is below the work function of the heated tungsten filament, the filament will emit electrons and at the same time ionize the cesium gas, generating a plasma which is relatively homogenous. Knechtli and Wada (7) have done considerable work on this type of plasma generation. Kino (8) has also used a similar scheme. In his tube, Fig. (3), a spiral heater was used, and due to the fields set up across the spiral, it was necessary to make all measurements during the time when power was not applied to the heater. By use of a flat ribbon, it is hoped to be able to reduce the field of the heater sufficiently so that measurements may be taken continously while applying a d.c. voltage to the heater.

Work on plasma microwave amplifier tubes has been carried on by several authors, (8), (9), (12), (13), (14), and (15). The major difference between the operation of the tube proposed here and the work of some previous authors is in the manner of coupling the energy into the device. Boyd, Field, and Gould, (9) studied plasma oscillations and growing plasma waves using a mercury arc discharge for a plasma, coupling the input R. F. signal to the electron beam, and thence to the plasma. Fig. (2) is a sketch of the device they used. Allen and Kino (8) studied the interaction of an electron beam with a fully ionized plasma using a cesium plasma and coupling the input R. F. signal to the electron beam, and thence to the plasma. Fig. (3) is a sketch of the device they

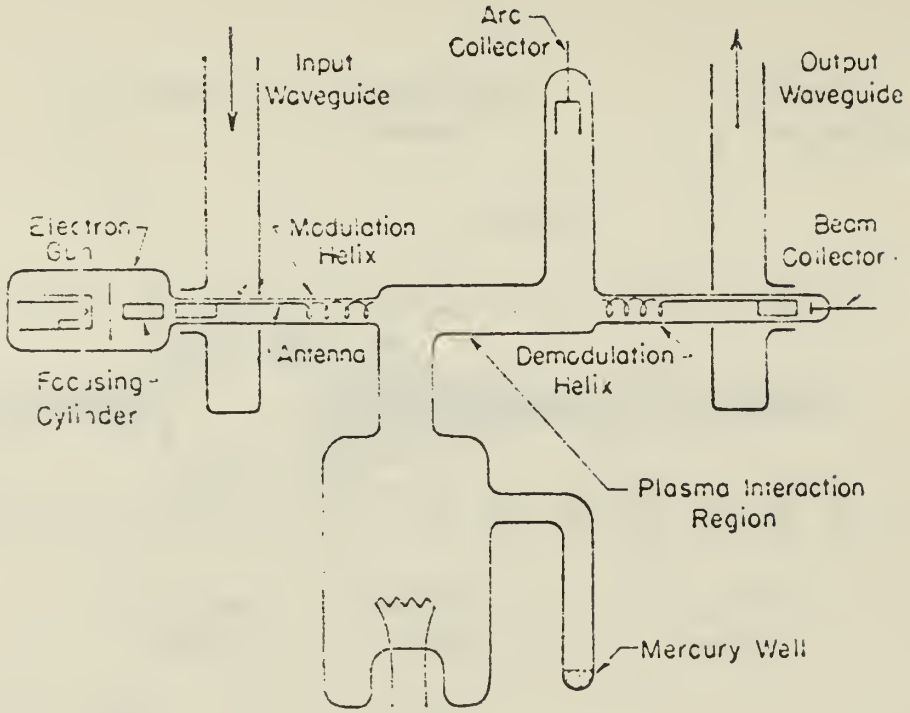
Arc
Collector
Input
Waveguide
Output
Waveguide
Electron
Gun
Modulation
Helix
Beam
Collector
Antenna
Demodulation
Helix
Focusing
Cylinder
Plasma Interaction
Region
Mercury Well

Fig. (2)

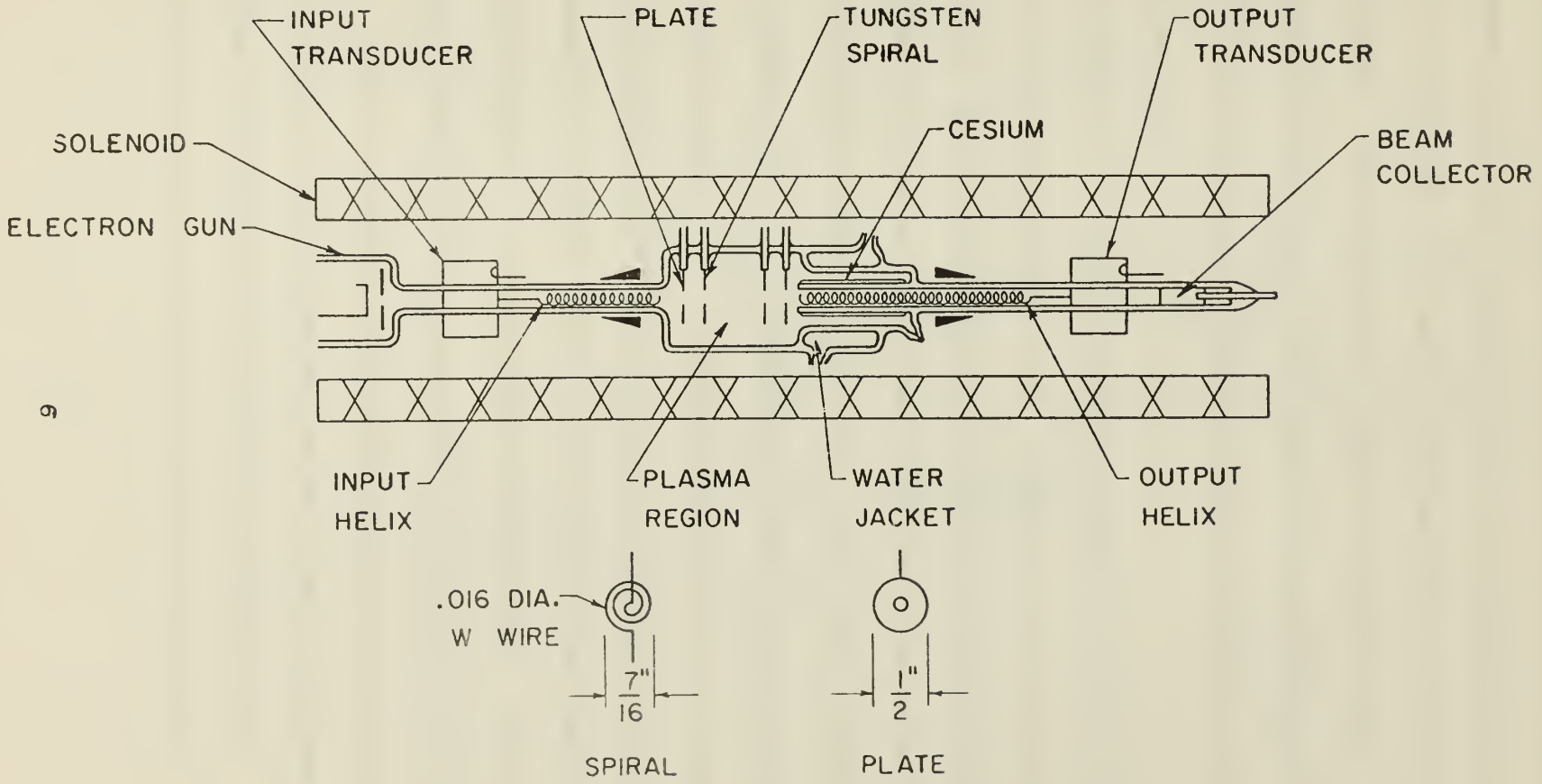
INPUT TRANSDUCER
PLATE
TUNGSTEN SPIRAL
OUTPUT TRANSDUCER
SOLENOID
CESIUM
BEAM COLLECTOR
ELECTRON GUN
INPUT HELIX
PLASMA REGION
WATER JACKET
OUTPUT HELIX
.016 DIA. W WIRE
7/16"
1/2"
SPIRAL
PLATE

Fig. (3)

used. Paik (12) used a coupled mode approach to study the coupling of modes between a slow wave mode and a helix. The experimental work he reported on was done with a device as shown in Fig. (4) which used a mercury plasma. He excited only one mode by careful coupling, using a selective mode coupler. This device did not include an electron beam, and his theoretical and experimental work was limited to the case of no magnetic field.

B.M. Bulgakov, et al. (13) studied slow waves in a helix - plasma column with an arbitrary magnetic field. This did not include any experimental work, and the final dispersion plots they developed showed discontinuities in the curves, which one would not expect to see. This has caused some workers in the field to question their results.

E. V. Bogdanov, et al. (14) studied very nearly the same problem as Boyd, Field, and Gould (9). The device they used for experimental work, although physically different, used an arc discharge type of plasma generator and coupled the input R. F. energy to an electron beam, and the output R. F. energy from the electron beam. The significant thing about this work is they were able to obtain gain from 25 cm. up to 3 cm. This was possible because they used an arc discharge to generate the plasma, and by increasing the arc current could generate a dense plasma, which was then contained by a magnetic field.

Work on an experimental X band tube has been carried out by

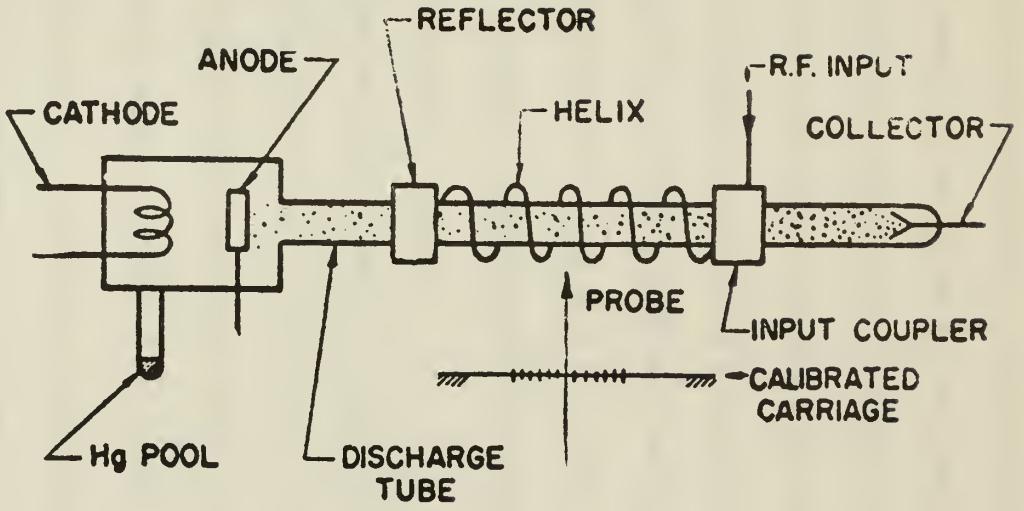
REFLECTOR
ANODE
R.F. INPUT
CATHODE
HELIX
COLLECTOR
PROBE
INPUT COUPLER
CALIBRATED
CARRIAGE
Hg POOL
DISCHARGE
TUBE

Fig. (4)

Microwave Associates, Burlington, Massachusetts.[1] This is a mercury device, again coupling the signal via an electron beam. Elcon Laboratory, Cambridge, Massachusetts is working on a device using the fast wave, designed to utilize the negative conductance of the plasma. All other devices proposed to date have used the slow wave mechanism. General Electric Ltd., Wembly England, has reported[1] a plasma X band unit which develops 60 db of gain in a six cm. tube. Philips Research Laboratories, Eindhoven, Netherlands has reported[1] a helix coupled tube giving 19 db gain at four Gc.

In all of the preceding devices coupling of the input signal to the device was accomplished by coupling as in a conventional traveling wave tube, to an electron beam with a helix, and then using the wave propagated on the beam to couple to the plasma. As a result of this, in the experimental work performed to date it has not been possible to couple directly to a backward wave plasma mode. It is anticipated that with the experimental device proposed, Fig. (1), it will be possible to investigate backward wave modes by direct coupling, as shown in Fig. (5).

[1] M. Meisels, Plasma Amplifiers Move Closer to Hardware Stage, Microwaves, pp 4-6, Jan. 1963

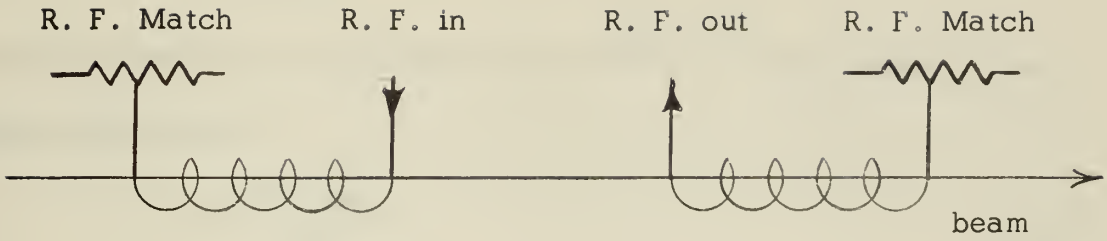

Fig. 5

If energy is coupled into and out of the plasma in this fashion, then if interaction with the electron beam is observed, it must necessarily be interaction with a backward wave. Of course, care must be exercised to ascertain whether this interaction occurs in the helix or in the drift region.

In considering the specific problem of coupling electromagnetic energy to a plasma column, it is perhaps worthwhile to review the work done in studying propagation on an electron beam. Hahn (10) and Ramo (11) considered a drifting, ion-neutralized cylindrical electron beam in an infinite axial magnetic field and found that in general there are two space charge waves, the propagation equation being.

$$\omega_p^2 - (\omega - \beta u_0)^2 = 0 \qquad (1.1)$$

for the one dimensional case, where

$$\omega_p^2 = -\eta \frac{\rho_o}{\epsilon_o} \tag{1.2}$$

$$\eta = \frac{e}{m}$$

and all quantities are assumed to have $e^{j(\omega t - \beta z)}$ dependence. Thus, the solutions are;

$$\beta = \frac{\omega \pm \omega_p}{u_o} \tag{1.3}$$

If u_o is zero, this one dimensional ion-neutralized electron beam does not propagate space charge disturbances. Trivelpiece (6) has shown however, that a finite u_o is not essential to the propagation of space charge disturbances when the beam has a finite transverse geometry.

Rigrod and Lewis (3) considered the problem of an electron beam under Brillouin flow conditions and found two types of space charge wave propagation, one involving a perturbation of the average charge density, and the other surface rippling. Brewer (4) considered the more general case of an arbitrary magnetic field.

2. Statement of the problem.

In order to study the coupling of R.F. energy between a helix slow wave structure and a plasma column, it is desirable to determine the $\omega - \beta$ plot or Brillouin diagram for the proposed circuit. This provides

all the information required to forecast the performance in interaction with electron beams, except knowledge of the actual field amplitudes involved, ref. Beck (1).

The term plasma as used here denotes a partially ionized gas which is electrically neutral in any macroscopic volume in the absence of disturbances. Further, for this discussion it has been assumed the ions are stationary, and the electrons have no random velocities and suffer no collisions. The neutral gas molecules are assumed to play no part in the process studied. It is felt this is a reasonable model for the plasma. Fig. (6) shows the basic configuration of the problem. The helix slow wave structure has been appproximated by the sheath helix model.

3. Analytical Solution.

Trivelpiece (6), has solved the problem of a plasma filled cylindrical waveguide in an infinite axial magnetic field, starting with the basic Maxwell equations. He further considers the finite magnetic field case where he neglects the a.c. magnetic fields, (quasi-static approximation). He presents, for the finite magnetic field case, the development of a complex dielectric tensor, to take into account the effects of the plasma in a finite magnetic field. This is:

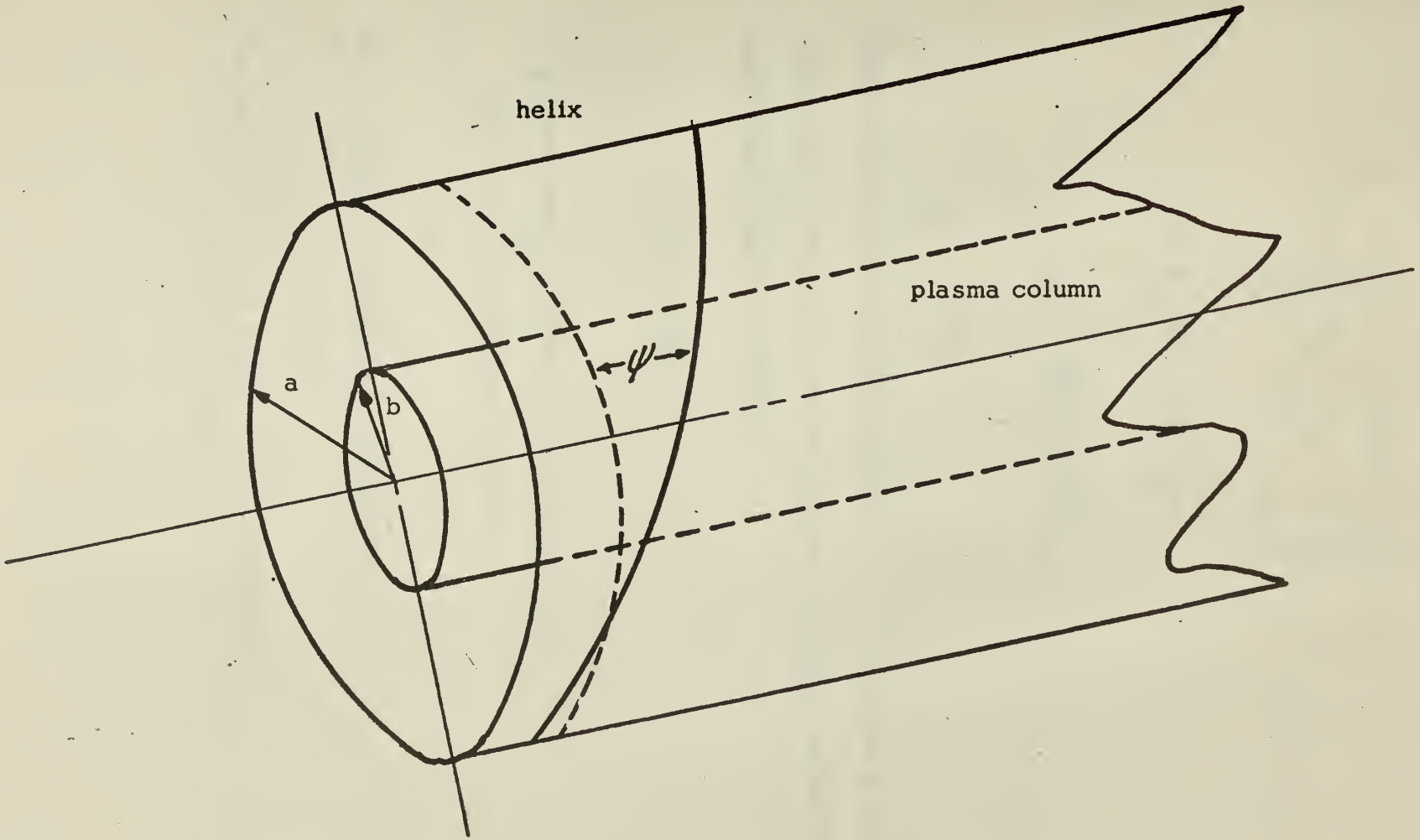

Fig. 6

$$\underline{\underline{\epsilon}} = \epsilon_o \begin{Vmatrix} \epsilon_{rr} & j\epsilon_{r\theta} & 0 \\ -j\epsilon_{\theta r} & \epsilon_{\theta\theta} & 0 \\ 0 & 0 & \epsilon_{zz} \end{Vmatrix} \tag{3.1}$$

$$\epsilon_{rr} = \epsilon_{\theta\theta} = 1 - \frac{\omega_p^2}{\omega^2 - \omega_c^2} \tag{3.2}$$

$$\epsilon_{r\theta} = \epsilon_{\theta r} = \frac{(\omega_c)\ \omega_p^2}{(\omega)\ (\omega_c^2 - \omega^2)} \tag{3.3}$$

$$\epsilon_{zz} = 1 - \frac{\omega_p^2}{\omega^2} \tag{3.4}$$

Making the quasi-static approximation, i.e. setting the a.c. magnetic fields to zero, we may solve the problem of matching between the helix and plasma column as follows:

$$\nabla \times \bar{E} = -j\omega\bar{B} = 0 \tag{3.5}$$

$$\therefore \bar{E} = -\nabla\phi$$

This approximation is presumed good for V^2 phase $<< c^2$

Now, for the equivalent dielectric,

$$\nabla \cdot \bar{D} = \nabla \cdot (\underline{\underline{\epsilon}} \cdot \bar{E}) = 0 \tag{3.6}$$

which suggests the differential equation

$$\nabla \cdot \underline{\underline{\epsilon}} \cdot \nabla\phi = 0 \tag{3.7}$$

The solution to which in cylindrical coordinates is:

$$\frac{1}{r}\frac{\partial}{\partial r}\left[r\,\epsilon_{rr}\frac{\partial\phi}{\partial r}+j\epsilon_{r\theta}\frac{1}{r}\frac{\partial\phi}{\partial\theta}\right]$$

$$+\frac{1}{r}\frac{\partial}{\partial\theta}\left[-j\epsilon_{\theta r}\frac{\partial\phi}{\partial r}+\epsilon_{\theta\theta}\frac{1}{r}\frac{\partial\phi}{\partial\theta}\right] \tag{3.8}$$

$$+\frac{\partial}{\partial_z}\left[\epsilon_{zz}\frac{\partial\phi}{\partial_z}\right]=0$$

In general one may assume a solution of the form

$$\phi = R(r)\,e^{-jn\theta}e^{-j\beta z} \tag{3.9}$$

However, we shall restrict ourselves to the case of no variation in θ (i.e. $n = 0$). This is not essential, but will simplify the analysis. Also this is the case of greatest practical importance. This then leads to the partial differential equation

$$\frac{1}{r}\frac{\partial}{\partial r}\left(r\frac{\partial\phi}{\partial r}\right)+\frac{\epsilon_{zz}}{\epsilon_{rr}}\frac{\partial^2\phi}{\partial_z^{\,2}}=0 \tag{3.10}$$

and solve

$$\frac{1}{r}\frac{d}{dr}\left(r\frac{dR}{dr}\right)-\beta^2\frac{\epsilon_{zz}}{\epsilon_{rr}}R=0 \tag{3.11}$$

and now let

$$\Gamma=-\beta^2\frac{\epsilon_{zz}}{\epsilon_{rr}}=-\beta^2\frac{1-(\omega_p^{\,2}/\omega^2)}{1-[\omega_p^{\,2}/(\omega^2-\omega_c^{\,2})]} \tag{3.12}$$

The solution to this equation, then is: $0 < r < b$

$$E_z = AJ_0(\Gamma r)e^{j(\omega\epsilon-\beta_z)} \tag{3.13}$$

$$E_r = -A \frac{j\Gamma}{\beta} J_1(\Gamma r) e^{j(\omega t - \beta_z)}$$

$$H\phi = -A \frac{j\Gamma\omega\underline{\epsilon}}{\beta^2} J_1(\Gamma r) e^{j(\omega t - \beta_z)} \qquad (3.13)$$

and for $b \leq r \leq a$

$$E_z = \left[BI_o(\beta r) + CK_o(\beta r)\right] e^{j(\omega t - \beta_z)}$$

$$Er = j\left[BI_1(\beta r) - CK_1(\beta r)\right] e^{j(\omega t - \beta_z)} \qquad (3.14)$$

$$H\phi = \frac{j\omega\underline{\epsilon}}{\beta} \left[BI_1(\beta r) - CK_1(\beta r)\right] e^{j(\omega t - \beta_z)}$$

and with suitable matching at the boundaries, we may reduce the above to:

$$\frac{\epsilon_{rr}}{\beta a} \frac{J_1(\Gamma a)}{J_o(\Gamma a)} = \qquad (3.15)$$

$$\frac{I_1(\beta a)\left[K_o(\beta b) + FK_1(\beta b)\right] + K_1(\beta a)\left[I_o(\beta b) - FI_1(\beta b)\right]}{-I_o(\beta a)\left[K_o(\beta b) + FK_1(\beta b)\right] + K_o(\beta a)\left[I_o(\beta b) - FI_1(\beta b)\right]}$$

where F is a function of the admittance Y_s of the sheath helix, defined as:

$$F = -\frac{j\omega\epsilon_o}{\beta Y_s} \qquad (3.16)$$

Y_s is the admittance of the helix. The expression for Y_s is given by Hutter (2) as:

$$Y_s = \frac{-j\frac{\omega\epsilon_0}{\beta}\frac{I_0(\beta a)}{I_1(\beta a)} + \frac{K_0(\beta a)}{K_1(\beta a)} - \frac{K_1(\beta a)}{K_0(\beta a)}\left(\frac{ka}{\beta a}\right)^2 \cot^2\psi}{\left(\frac{ka}{\beta a}\right)^2 \cot^2\psi} \qquad (3.17)$$

using the sheath helix approximation. It should be noted that inherent in use of this expression for the admittance of the sheath helix is the further assumption of a free space TE mode within the helix. The use of a TE mode in addition to the TM mode is required to match the boundary conditions at the helix.

Paik, (12) has developed an analysis using the coupled mode approach for a helix-plasma column in the zero magnetic field case. The above general expression, equation (3.15) may be shown to reduce to that of Paik in the zero magnetic field case, (let ω_c go to zero).

Fig. 14 shows an $\omega-\beta$ plot for the zero and infinite magnetic field case, with the parameters defined as follows:

$C_1 = k_p a \cot\psi$

$C_2 = b/a$

$C_3 = k_c a \cot\psi$

$x = pa$

$y = ka \cot\psi$

where $k = \omega/C$

C = the velocity of light

The data was obtained by use of a digital computer. The general program and necessary function subroutines are given in appendix I.

Fig. (7) and Fig. (9) thru Fig. (17) show $\omega - \beta$ plots for various parameters in the general magnetic field case. Fig. (7) shows the principle modes, as well as a few of the higher order modes. These higher order modes result mathematically from the multiple roots of the Bessel functions, and represent higher order modes of operation. Since there are an infinite number of roots to the Bessel functions, there are an infinite set of these higher order modes in the regions where the propagation constant is real. A sample plot of this situation is shown in Fig. (8) for a typical case. The symbols used follow those of the computer program. Z is the right hand side of Eq. (3.15) and BB is the left hand side of this equation. This plot is for a fixed value of x. In the region where the propagation constant is imaginary, Z reduces to a function of two modified Bessel functions, usually represented as $I_n(x)$ which do not exhibit this multiplicity of roots, and therefore do not indicate higher order modes of operation in these regions.

4. Discussion.

The $\omega - \beta$ curves for the finite magnetic field case show several promising facets. The backward wave mode is an interesting phenomenon, and indicates the possibility of a backward wave oscillator.

Fig. (7) shows a detailed set of $\omega - \beta$ relationships for the case of $k_p a \cot \psi = 3.0$, $b/a = 0.8$, and $k_c a \cot \psi = 5.0$. Fig. (8) shows plots of the left hand and right hand sides of Eq. (3.15) vs $ka \cot \psi$ for $pa = 4.0$. The perturbations of the helix wave as shown in Fig. (7) indicate that considerable coupling exists between the helix and plasma for this finite magnetic field case. This is encouraging, and indicates that one might reasonably expect to couple the input and output energy directly to and from the plasma rather than coupling to the electron beam and thence to the plasma as has been done by previous workers, and this direct coupling to the plasma would thereby allow excitation of the backward waves as previously discussed.

The various modes of operation depicted in Fig. (7) are plasma modes, that is, they are not space harmonic modes of the helix, inasmuch as the sheath helix approximation does not include the space harmonics which exist with the actual helix. Therefore, in a solution which utilized a more exact representation for the helix one might expect to see in addition a coupling between the plasma and higher order helix modes. In the limiting case as the sheath helix goes over to a

conducting cylinder, these modes shown would be the various radial modes found by Trivelpiece, (6) and denoted as the $p_{o\nu}$ modes where $p_{o\nu}$ is the νth zero of the zero order Bessel Function of the first kind. From Fig. (8), we see that the solution at point a represents the perturbed helix wave, the solutions to the right of point a, the modes in the backward wave region, and those solutions to the left of a the modes in the forward wave region. For example the solution at point b represents the first plasma wave, and this point corresponds to the point b on Fig. (7). The solution at point e represents the first order solution of the backward wave region and corresponds to the point e on Fig. (7). The other points correspond as they are lettered. Thus we may see the mathematical generation of these higher order modes, and may visualize them as representing higher order radial modes. There are of course an infinite set of these modes, only a few of which have been shown.

The slight backward wave region of the perturbed helix mode indicates this device might have some promise as a backward wave oscillator. It is noted, however, that the bandwidth of any such device would be relatively narrow. The forward wave characteristics indicate that a forward wave amplifier might be designed to be quite broadband, however.

It should be noted that the higher order radial modes are probably

not particularly useful for interaction inasmuch as it would be difficult if not impossible to couple to them due to the reversal of field potential in the radial cross section which such a mode would represent.

Fig. (9) thru Fig. (16) show the effect of variations in ω_p and ω_c as well as the ratio of b/a. These curves are included to provide some insight into the effects of a variation of these parameters. First it is to be noted that for $\omega_p < \omega_c$ the lowest order plasma wave cuts off at ω_p, and for $\omega_c < \omega_p$ the plasma wave appears to cut off somewhere between ω_p and ω_c. The backward waves and helix wave approach as a limit ω_c when $\omega_c > \omega_p$, and approach as a limit ω_p when $\omega_p > \omega_c$. Further, the backward waves cut off at the $\sqrt{\omega_p^2 + \omega_c^2}$. The above observations are similar to those found by Trivelpiece (6) in the plasma - cylinder problem. The larger b/a, the more completely the plasma fills the helix. It is seen that this leads to more bandwidth in the backward wave region. Also, the knee of the curve is less sharp as the helix wave goes over into a backward wave mode. This one might expect since a larger b/a would lead one to expect tighter coupling between the helix and the plasma.

Fig. (17) shows a plot of the helix and plasma waves for the zero and infinite magnetic field case. The infinite magnetic field case shows a continuation of the effects noted previously. There appears to be a smooth transition to the zero magnetic field case as well. As ω_c

is decreased, the backward wave region, essentially between ω_p and $\sqrt{\omega_p^2 + \omega_c^2}$ becomes smaller and smaller, until in the limiting case there is no such region. The helix wave becomes more and more nearly like the uncoupled helix wave as ω_c is decreased, and finally for $\omega_c=0$ we see that the helix wave shows no backward wave region, and is only slightly perturbed by the plasma as may be seen by comparison with the free helix wave also plotted on the same figure. The plasma wave, which at values of $\omega_c > \omega_p$ appears to cut off at ω_p, cuts off at lower and lower frequencies as ω_c is decreased below ω_p and finally approaches the limit as shown for the zero magnetic field or $\omega_c = 0$ case.

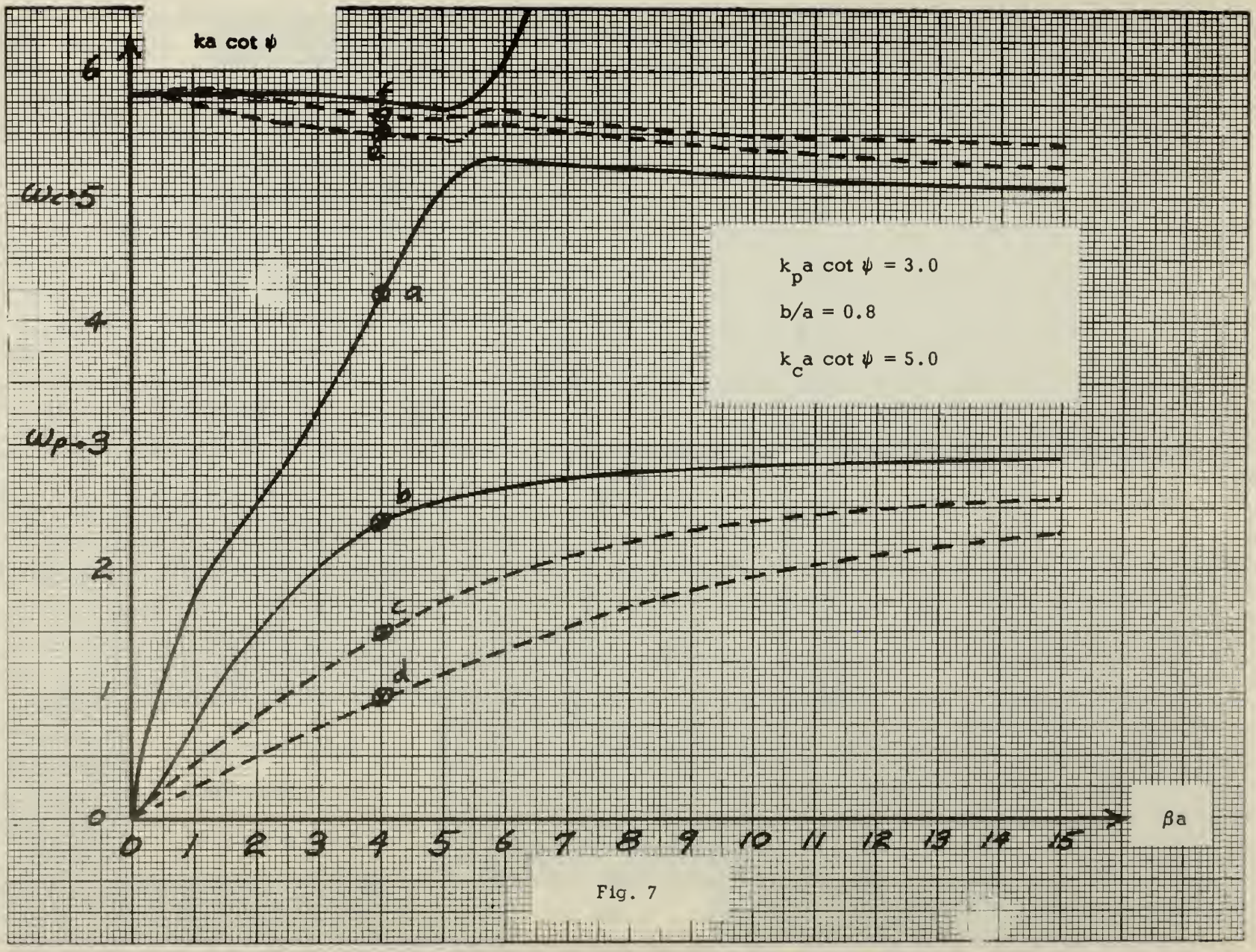
ka cot ψ
6
4
2
0
ω_c=5
ω_p=3
a
b
c
d
$k_p a \cot \psi = 3.0$
b/a = 0.8
$k_c a \cot \psi = 5.0$
0 1 2 3 4 5 6 7 8 9 10 11 12 13 14 15
βa

Fig. 7

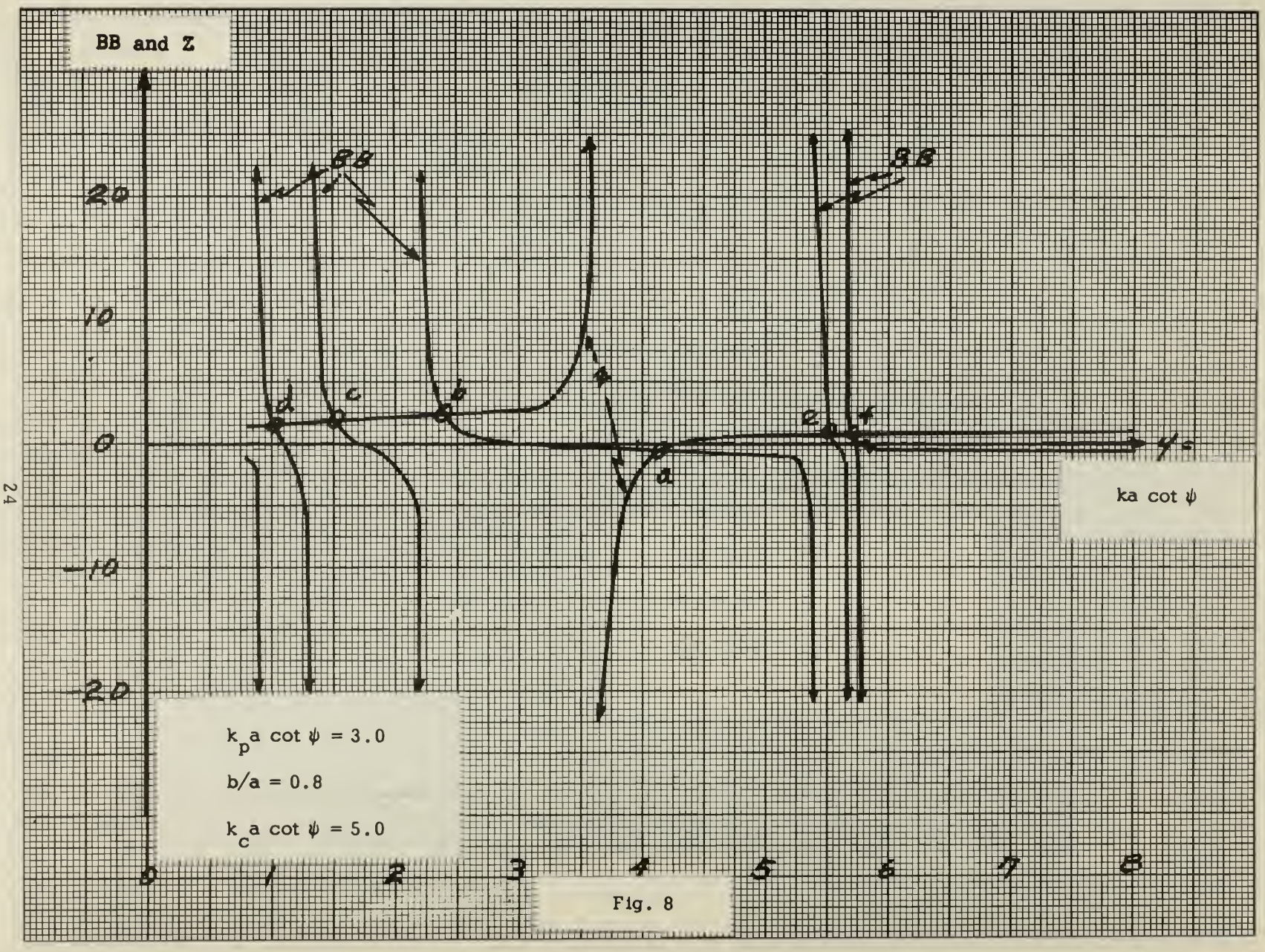
BB and Z
δθ
δθ
20
10
0
-10
-20
a
b
c
d
e
f
ka cot ψ
$k_p a \cot \psi = 3.0$
b/a = 0.8
$k_c a \cot \psi = 5.0$
0
1
2
3
4
5
6
7
8

Fig. 8

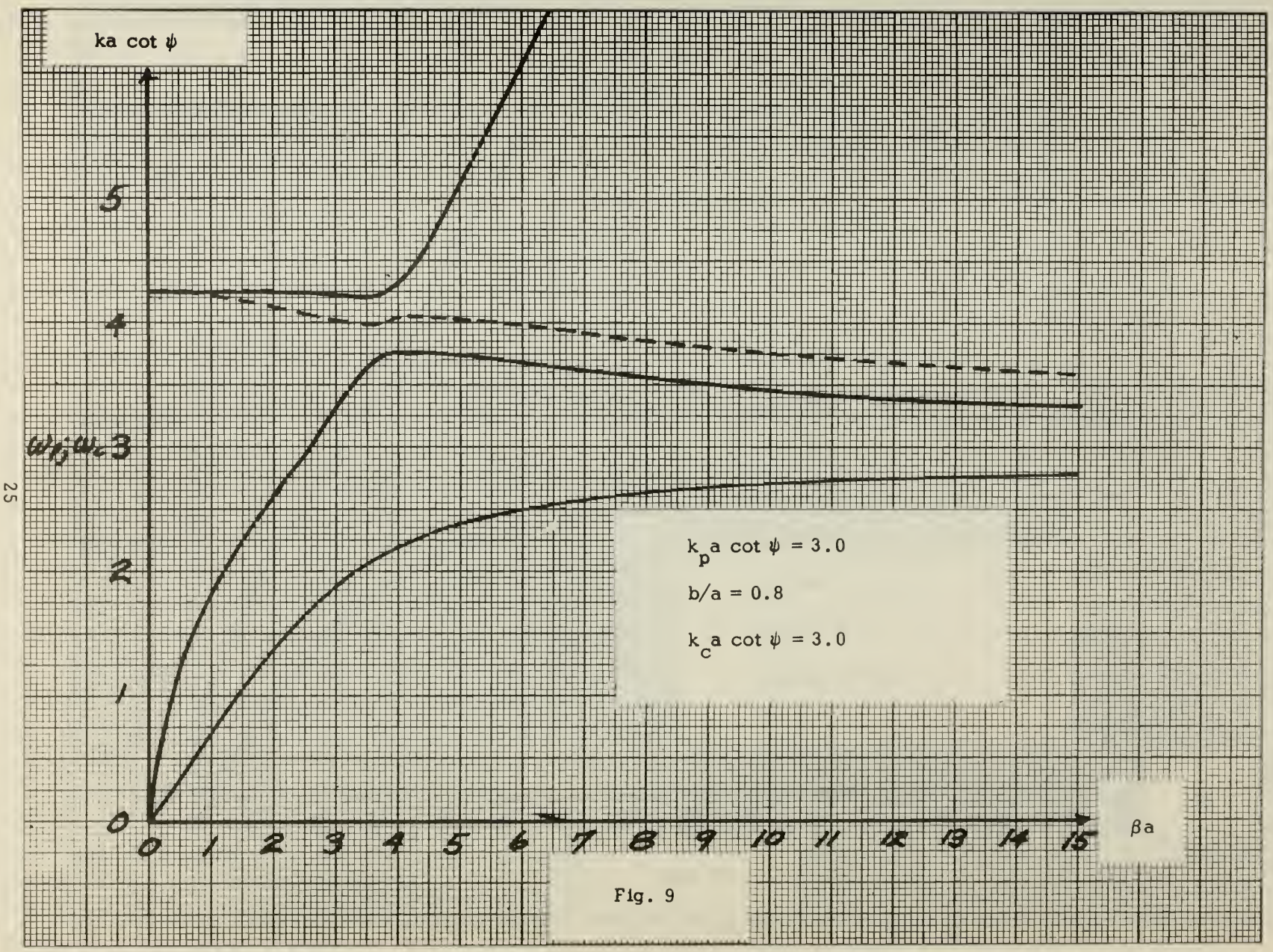
ka cot ψ
5
4
3
2
1
0
ω_b, ω_c
0 1 2 3 4 5 6 7 8 9 10 11 12 13 14 15
βa
$k_p a \cot \psi = 3.0$
b/a = 0.8
$k_c a \cot \psi = 3.0$

Fig. 9

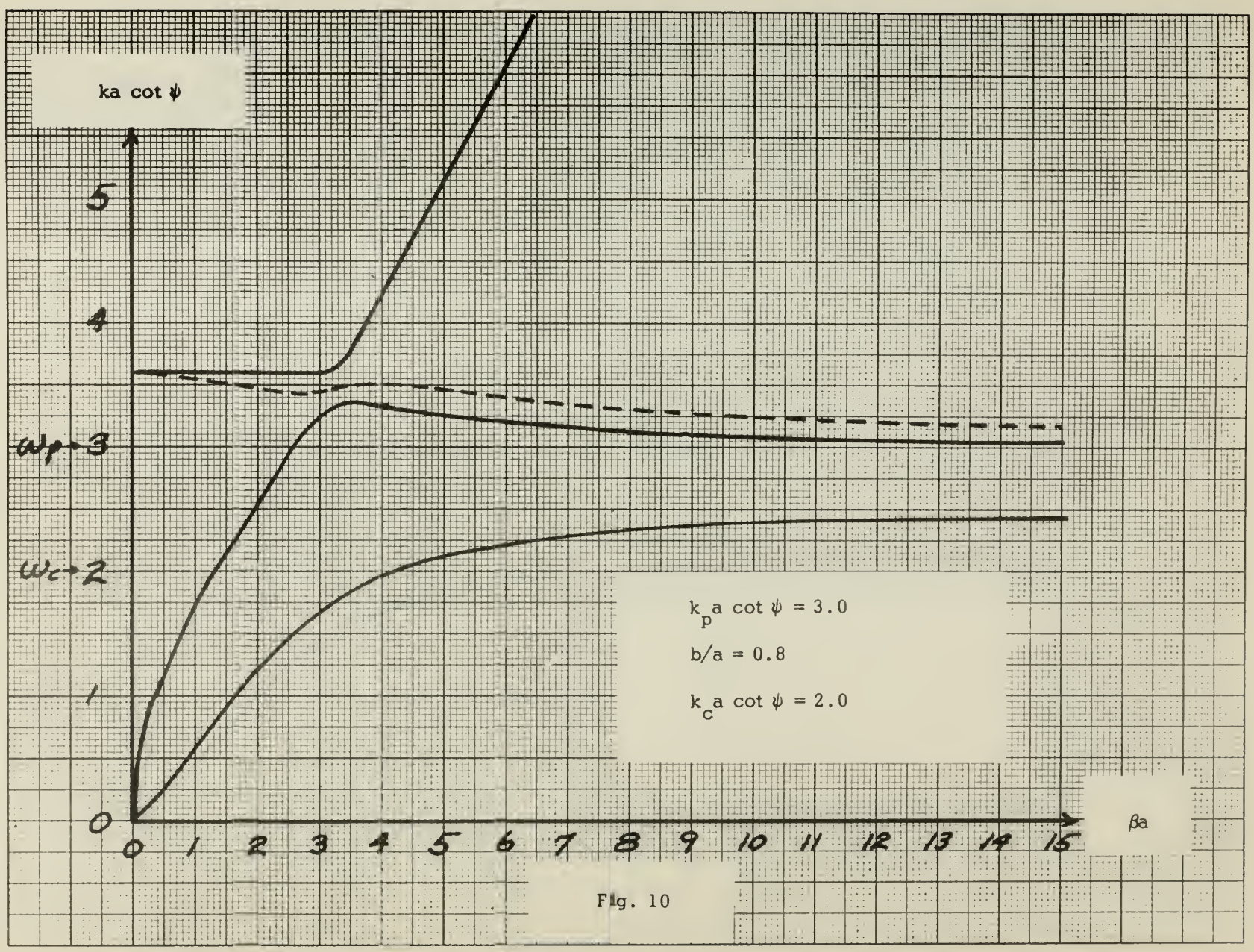
ka cot ψ
5
4
$\omega_p \to 3$
$\omega_c \to 2$
1
0
0 1 2 3 4 5 6 7 8 9 10 11 12 13 14 15
βa
$k_p a \cot \psi = 3.0$
b/a = 0.8
$k_c a \cot \psi = 2.0$

Fig. 10

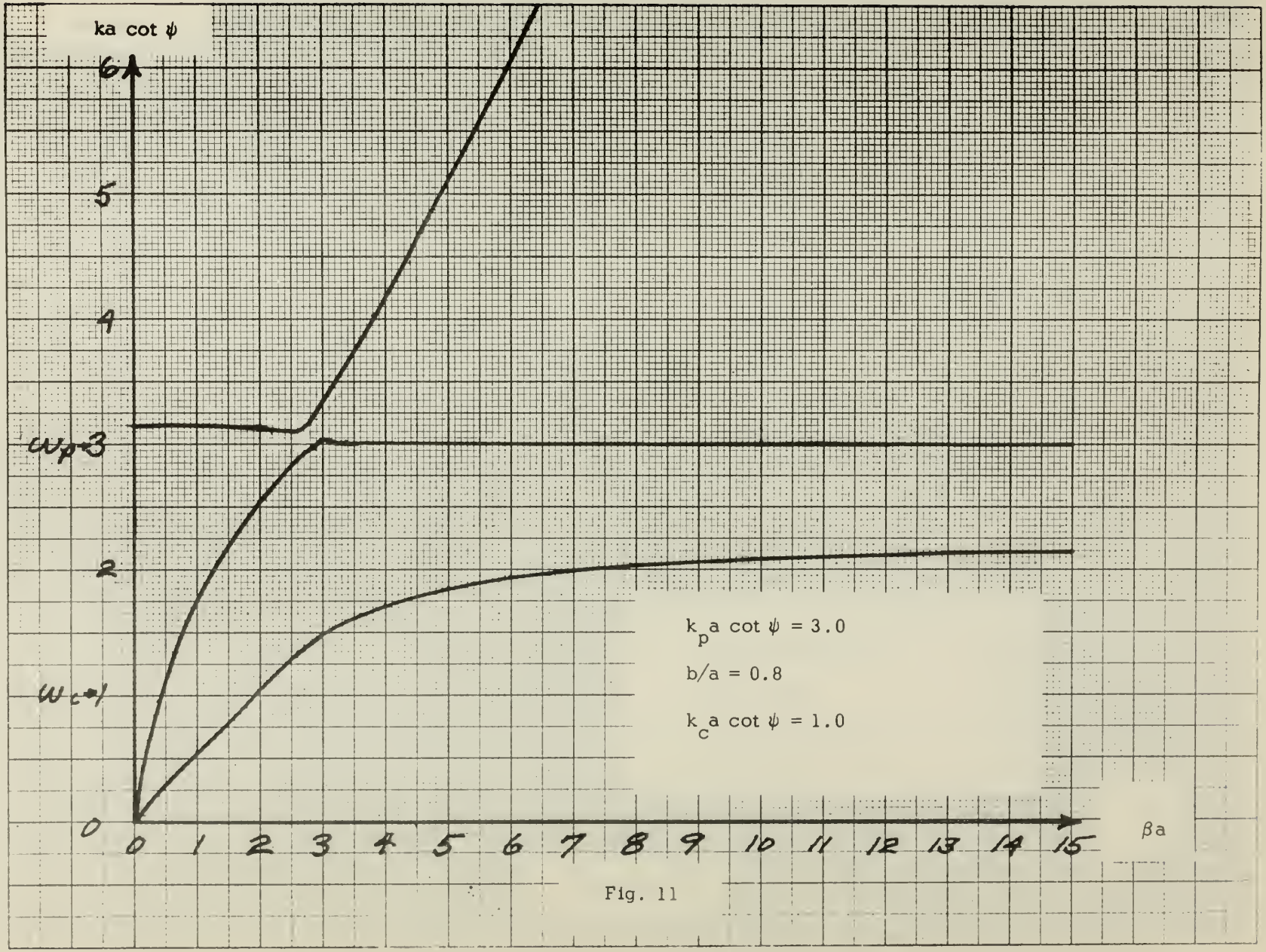
ka cot ψ
6
5
4
3
2
1
0
ω_p
ω_c
$k_p a \cot \psi = 3.0$
b/a = 0.8
$k_c a \cot \psi = 1.0$
0 1 2 3 4 5 6 7 8 9 10 11 12 13 14 15
βa

Fig. 11

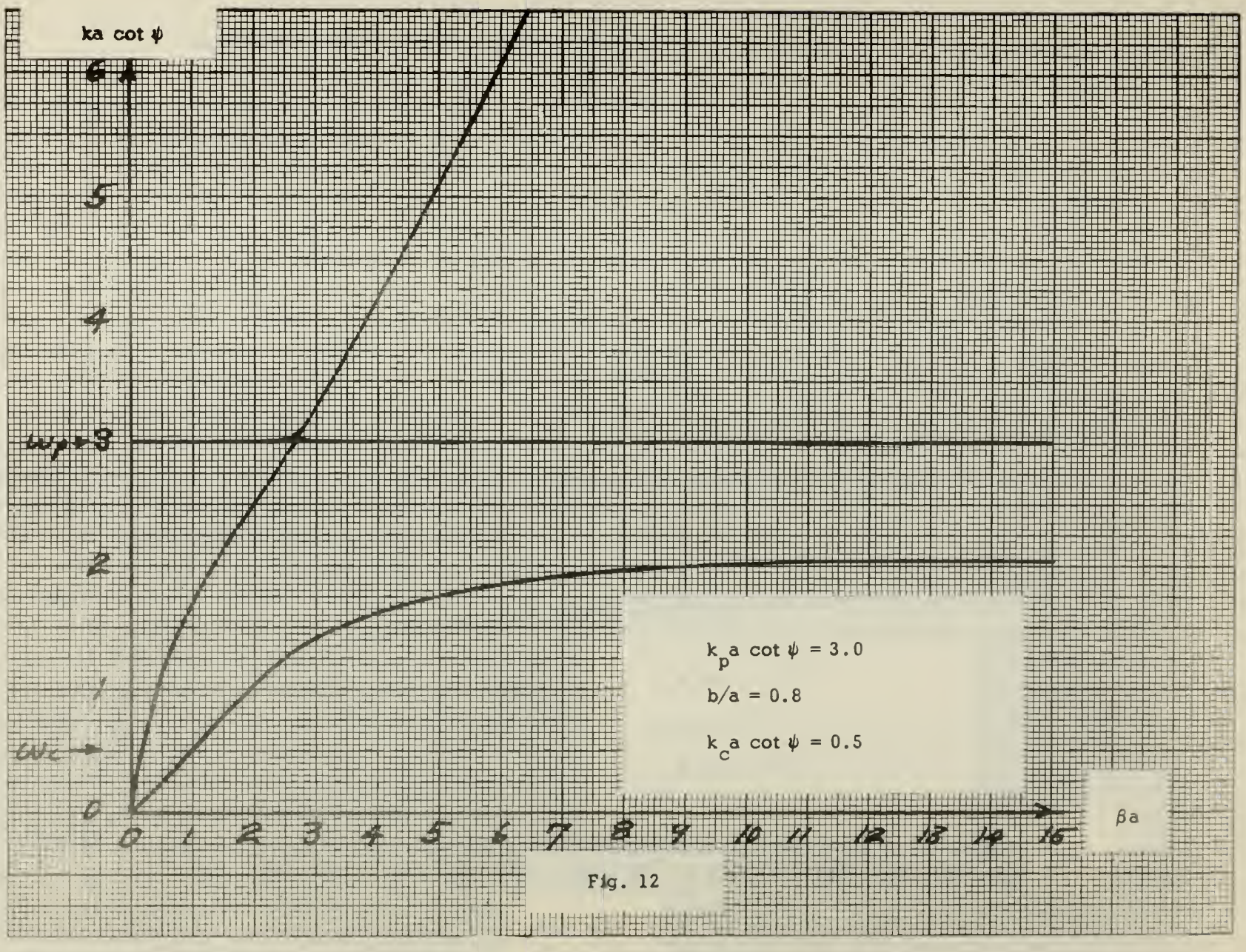
ka cot ψ
6
5
4
ω_p = 3
2
1
ω_c
0
0 1 2 3 4 5 6 7 8 9 10 11 12 13 14 15
βa
k_p a cot ψ = 3.0
b/a = 0.8
k_c a cot ψ = 0.5

Fig. 12

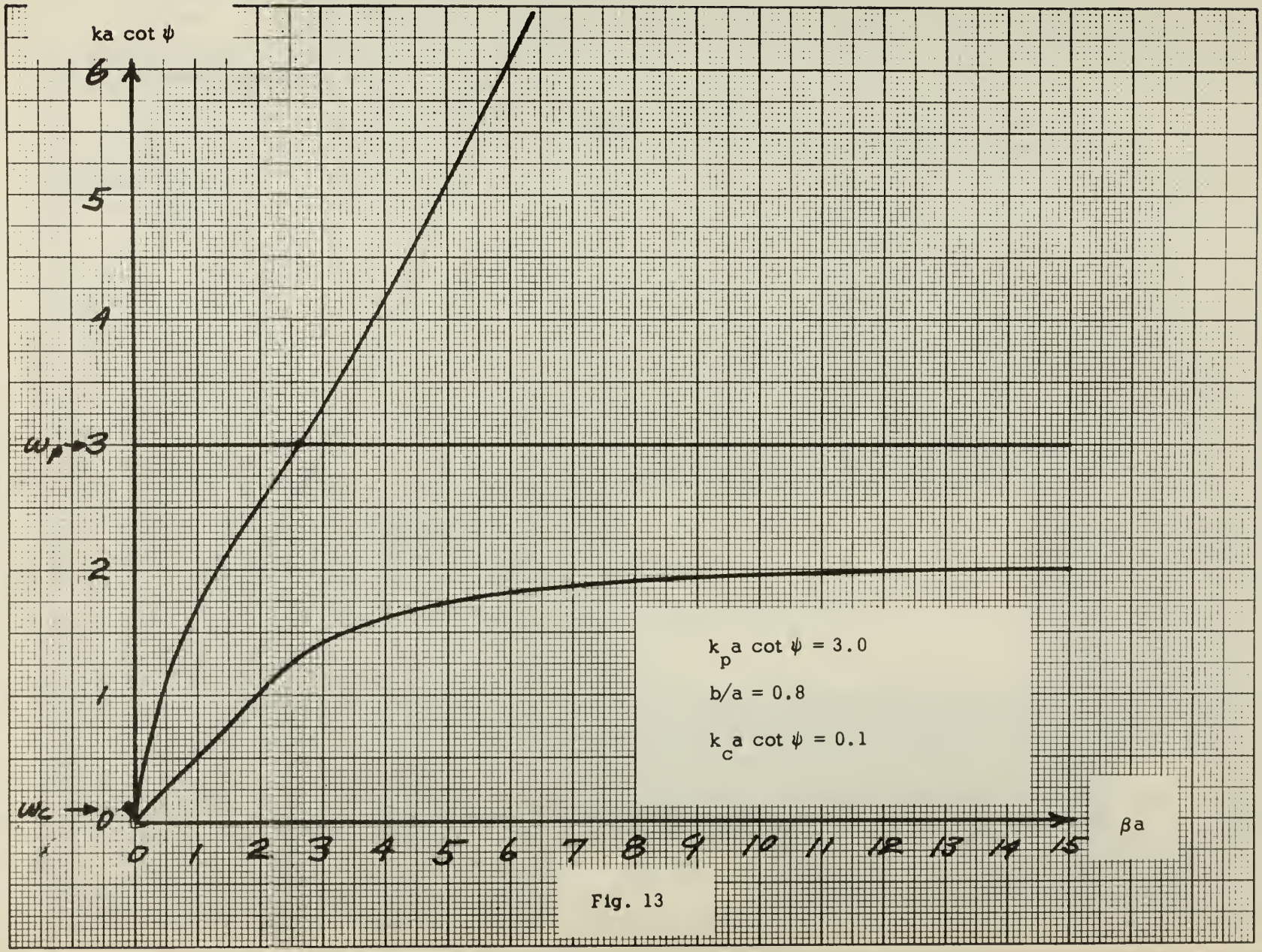
ka cot ψ
6
5
4
3
2
1
0
w_p
w_c
0 1 2 3 4 5 6 7 8 9 10 11 12 13 14 15
βa
k_p a cot ψ = 3.0
b/a = 0.8
k_c a cot ψ = 0.1

Fig. 13

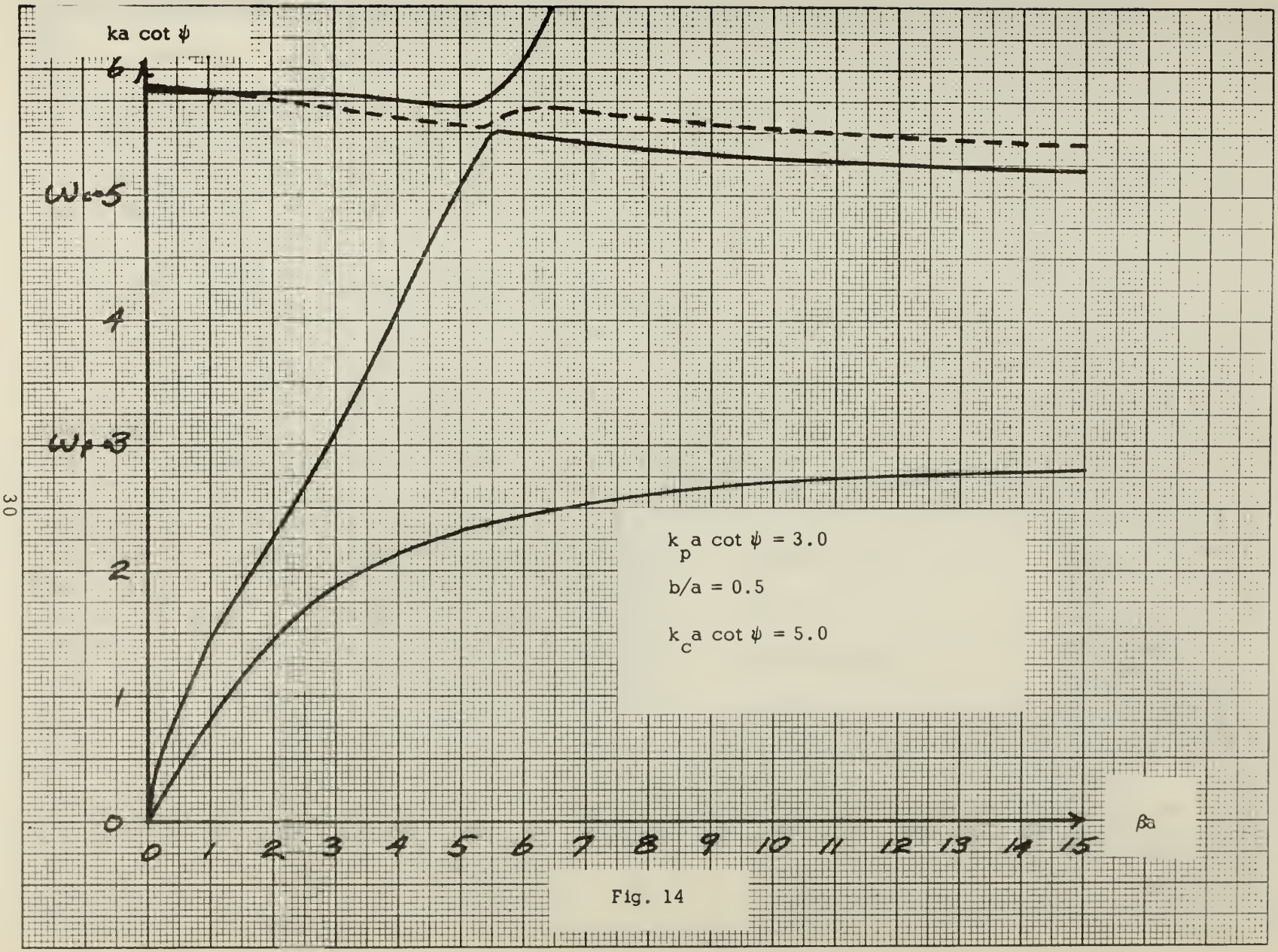
ka cot ψ
6
W=5
4
W=3
2
1
0
0 1 2 3 4 5 6 7 8 9 10 11 12 13 14 15
βa
k_p a cot ψ = 3.0
b/a = 0.5
k_c a cot ψ = 5.0

Fig. 14

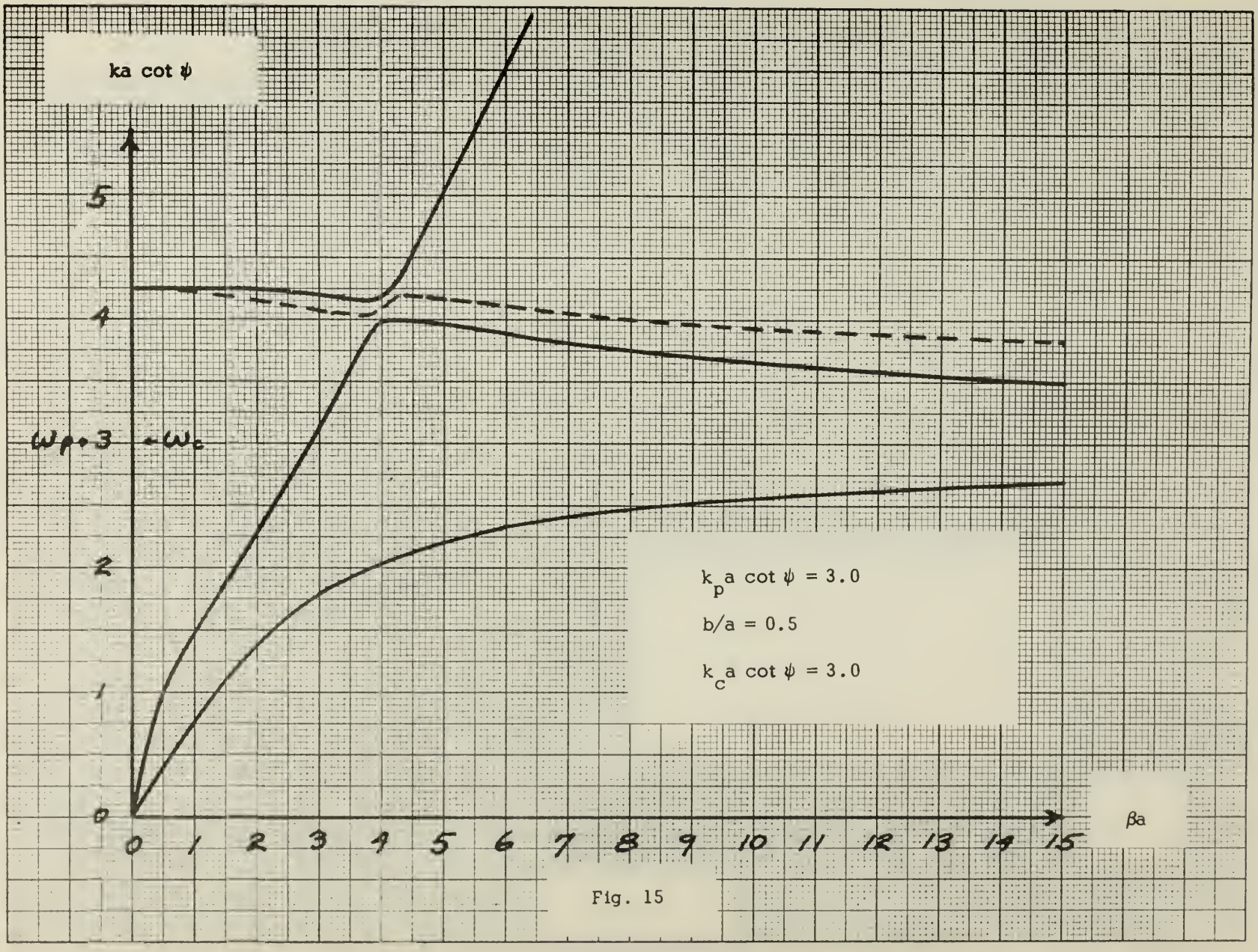
ka cot ψ
5
4
$\omega_p = 3$
ω_c
2
1
0
0 1 2 3 4 5 6 7 8 9 10 11 12 13 14 15
βa
$k_p a \cot \psi = 3.0$
b/a = 0.5
$k_c a \cot \psi = 3.0$

Fig. 15

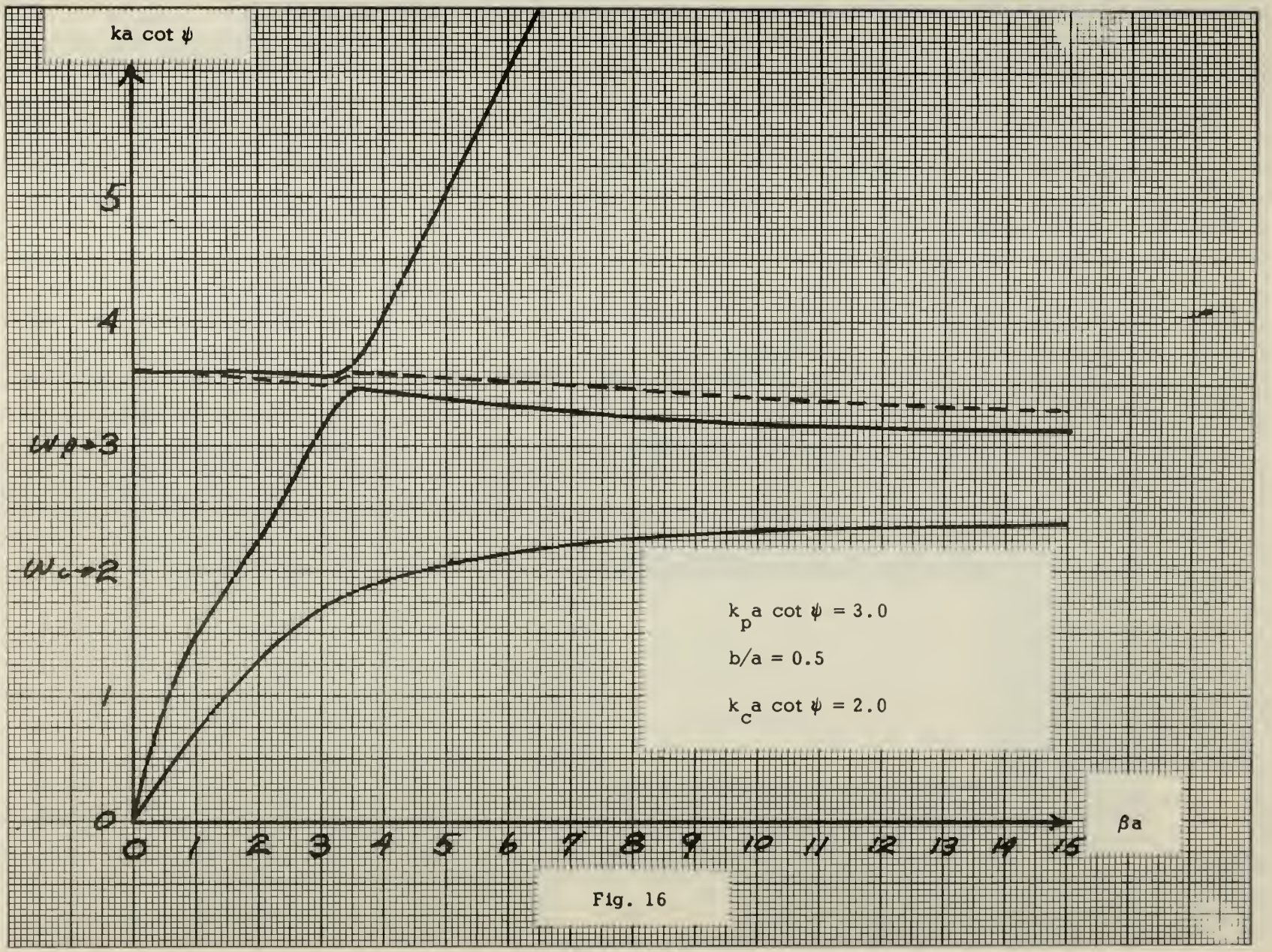
ka cot ψ
5
4
w_p=3
w_c=2
1
0
0 1 2 3 4 5 6 7 8 9 10 11 12 13 14 15
βa
$k_p a \cot \psi = 3.0$
b/a = 0.5
$k_c a \cot \psi = 2.0$

Fig. 16

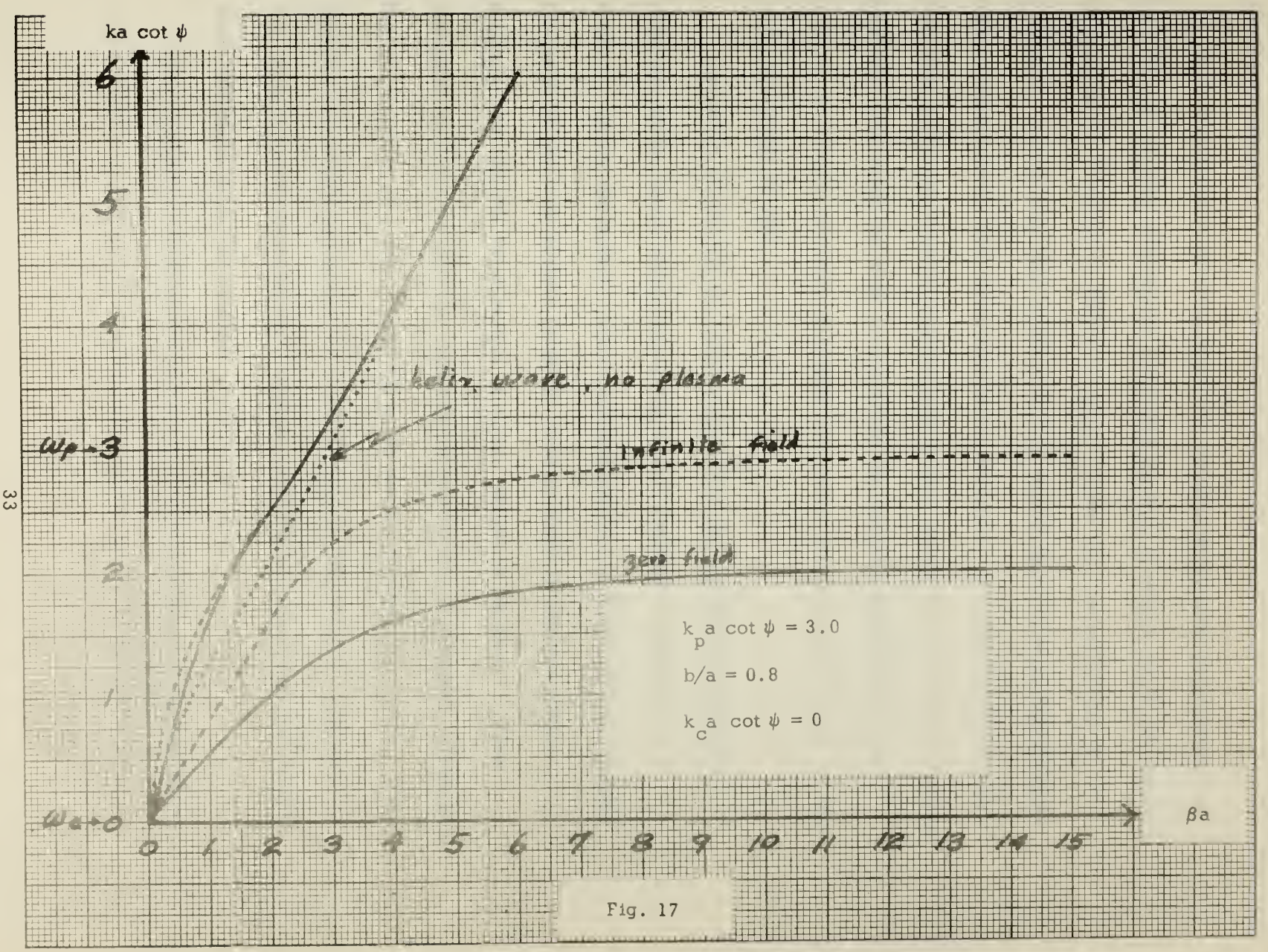
ka cot ψ
6
5
4
ωp=3
2
1
ωc=0
0 1 2 3 4 5 6 7 8 9 10 11 12 13 14 15
βa
helix wave, no plasma
infinite field
zero field
$k_p a \cot \psi = 3.0$
b/a = 0.8
$k_c a \cot \psi = 0$

Fig. 17

5. Conclusions.

In conclusion it appears from the results of the analysis presented here that a plasma microwave amplifier device in which the R. F. Energy is coupled to the plasma directly offers some real possibilities of success. It appears that such a device would have several advantages over conventional type traveling wave devices. Principally these are that one might reasonable expect high power operation in a small device, and that one might be able to alleviate the serious mechanical and cooling problems inherent in higher frequency microwave devices of the type presently in use.

However, it should be emphasized that the analysis presented contains three basic approximations which limit the validity of the theory. First, the quasi - static approximation is made, which should be good for the low values of beam voltage used in typical tubes. Second, the sheath helix model is used, which is believed to be a reasonable model within the limitations previously mentioned. Finally, the assumption of a free space TE mode within the helix is made. This assumption would appear to be justified since the solution obtained in the case of zero magnetic field agrees with Paik's analysis (12) which does not make this assumption.

The dispersion relationships of Fig. (9) thru Fig. (16) do not show any anomalous discontinuities as were found by B. M Bulgakov et al.

(13).

The data contained in this paper is not sufficient in itself to draw firm conclusions regarding the operation of a plasma microwave amplifier device, however. The ω-β diagram does not provide any information regarding the magnitudes of fields involved, and thus no insight into the interaction impedances involved. A theoretical study of interaction impedance should be an interesting and worthwhile project and is suggested as the subject for some future investigation.

6. Proposed Experimental Work.

After completing all connections for the experimental tube, it is proposed that the following experimental work be accomplished:

1. Make cold tests of impedance match to the helix, and determine the losses incurred in the helix couplers over a frequency range of at least 1.0 to 2.5 Gc.

2. Determine the $\omega - \beta$ relationships as indicated from the theoretical work.

4. Carry out electron beam interaction experiments.

5. Investigate the backward wave regions shown theoretically, this being of special interest. These experiments should be designed to determine the range and magnitude of self oscillation available as well as bandwidth optimization by variation of field strength and

plasma density.

In the experiments involving measurements of the R. F. interaction, measurements should also be made to determine the impedance levels, gain, or loss in the helix regions, and gain or loss in the drift region. Further, these experiments should be carried on over a wide range of magnetic fields, tube temperatures, and frequencies.

Care should be exercised to assure the cooling provided by the water jacket is adequate to maintain an effective temperature along the region so cooled. Fig. (18) shows a photograph of the laboratory equipment designed to work with the proposed tube. The magnet, tube, and heat sinks for the filament rectifiers are water cooled. Fig. (19) shows a block diagram of the proposed measurement setup.

The magnet is designed to provide an adjustable uniform field from 0 to 2000 gauss. The plasma generation filament supplies are designed to provide from two to six volts, and up to a maximum of 120 amps each. The rectifiers are rated at 250 amps., the transformer being the limiting element.

Fig. 18

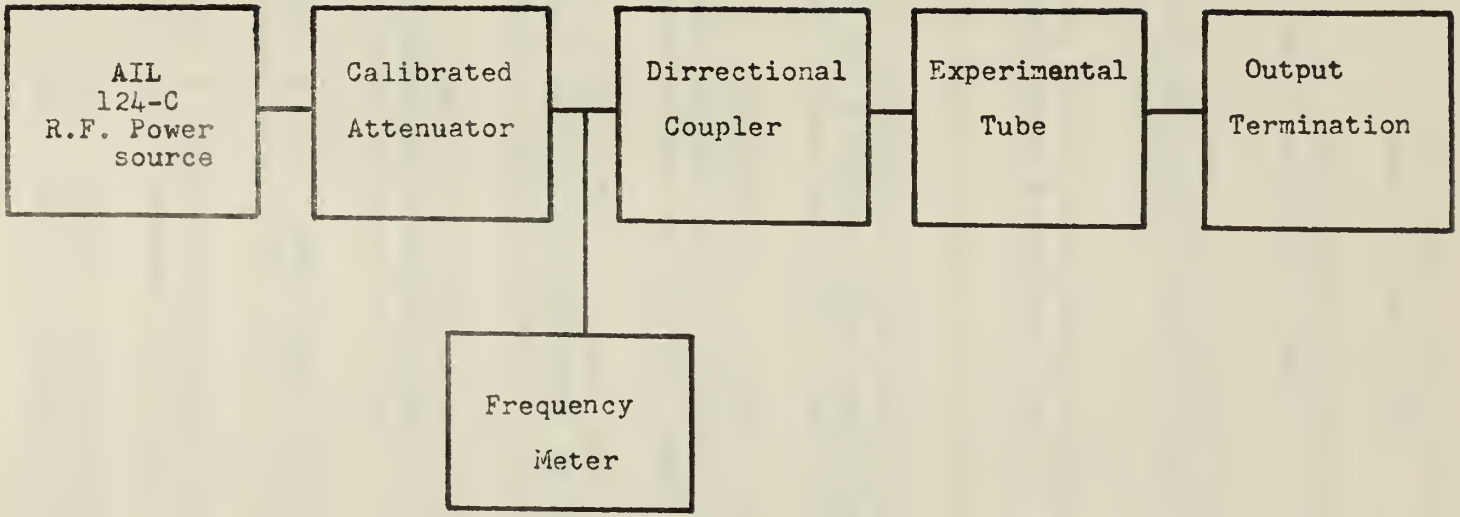
AIL
124-C
R.F. Power
source
Calibrated
Attenuator
Dirrectional
Coupler
Experimental
Tube
Output
Termination
Frequency
Meter

Fig. 19

BIBLIOGRAPHY

1. A. H. W. Beck, Space Charge Waves and Slow Electromagnetic Waves, Pergamon Press, 1958.

2. R. G. E. Hutter, Beam and Wave Electronics in Microwave Tubes, D. Van Nostrand Co., 1960.

3. W. W. Rigrod and J. A. Lewis, Wave Propagation along a Magnetically Focused Cylindrical Electron Beam, B. S. T. J., pp 399-416, March 1954.

4. G. R. Brewer, Some Effects of Magnetic Field Strength on Space-Charge Wave Propagation, Proc. I. R. E., pp 895-903, July 1956.

5. J. R. Pierce, Traveling-Wave Tubes, D. Van Nostrand Co., 1950.

6. A. W. Trivelpiece. Slow Wave Propagation in Plasma Waveguides TR. No. 7, Electron Tube and Microwave Lab., Calif. Inst. of Tech., Pasadena, Calif., May 1958.

7. R. C. Knechtli and J. Y. Wada, Generation and Measurement of Highly Ionized Quiesent Plasmas in Steady State. Physical Review letters, pp 215-217, March 1, 1961.

8. M. A. Allen and G. S. Kino, Beam Plasma Amplifiers, Technical Report, Microwave laboratory, W. W. Hanson Laboratories of Physics, Stanford University, July 1961.

9. C. D. Boyd, L. M. Field, and R. W. Gould, Excitation of Plasma Oscillations and Growing Plasma Waves. Physical Review, pp 1393-1394, Feb. 15, 1958.

10. Hahn, W. C., "Small Signal Theory of Velocity-Modulated Electron Beams," Gen. Elec. Rev., pp 591-596, June 1939.

11. Ramo, S. "Space Charge Waves and Field Waves in an Electron Beam," Phys. Review, pp 276-283, August 1939.

12. S. F. Paik, Coupling of Modes Between A Slow-Wave Plasma Mode and a Helix, Journal of Applied Physics, pp 2468-2473, August 1962.

13. B. M. Bulgakov, V. P. Shestopalov, L. A. Shishkin, and I. D. Yakmenko, Slow Waves in a Spiral Waveguide with a Plasma, Soviet Physics, pp 791-801 1960/1961.

14. E. V. Bogdanov, V. J. Kislov, Z. S. Tchernov, Interaction Between an Electron Stream and Plasma, Symposium on Millimeter Wave Generation, Polytechnic, Institute of Brooklyn, pp 57-67; 1959.

15. M. Meisels, Plasma Amplifiers Move Closer To Hardward Stage, Microwaves, pp 4-6; January, 1963.

```
..JOB  JONES GRAPH CN 8  7
       PROGRAM JONES3
       PRINT 1
 1     FORMAT (12H TUBE DESIGN  )
 16    FORMAT(18H IMAGINARY GAMMA     )
 15    FORMAT (2X,6(2X,E15.8))
  5    FORMAT (2X,6(2X,E15.8))
 17    FORMAT(18H X,Y,HZ,HZY,F,HBB    )
 7     FORMAT(5X,3(5X,E15.8))
       PRINT 17
       DIMENSION X1(900),Y1(900)
       DIMENSION T(1000)
C      Y= KACO+ PSI
C      X= PA
C      CON1 =KPACOT(PS1)
C      CON2=B/A
C      F= -J(OMEGA)(EPSOION ZERO)/P(YS)
       CON3=5.0
       CON2=0.8
       CON1=3.0
       PRINT 7,CON1,CON2,CON3
       II=50
       LL=200
 43    CONTINUE
       DO 40 M=LL,15000,II
       L=M
       KA=-1
 3     DO 50 K=5,375,1
 53    X=FLOATF(K)/25.0
       N=L
       AA=CON2*X
       A0=BESI(0.0,X)
       A1=BESI(1.0,X)
       CALL BESS(0,X,2,B0,T)
       CALL BESS(1,X,2,B1,T)
       C0=BESI(0.0,AA)
       C1=BESI(1.0,AA)
       CALL BESS(0,AA,2,D0,T)
       CALL BESS(1,AA,2,D1,T)
 4     DO 60 J=N, 15000, 1
       Y=FLOATF(J)/2000.0
       L=J
       A=.0000001
       IF(SENSE SWITCH 2) 102,103
 102   Y=2.*Y1(KK-1)-Y1(KK-2)-A
 103   AB=Y/X
       Q=(CON1/Y)
       RA=Y**2.0
       RB=CON3**2.0
       RC=RA-RB
 51    RD=(CON1)**2.0/RC-1.0
       RR=1.0-(CON1)**2.0/RC
       GAP = ABSF(((Q)**2.0)-1.0)/RD)**0.5
       GAB = CON2*X* GAP
       XNUM1 =(AB)** 2.0
       DEN1=A0/A1 +B0/B1 - (B1/B0)*XNUM1
       F =XNUM1/DEN1
       IF (SENSE SWITCH 1) 101,120
 120   IF(Q-1.0) 12,13,13
  12   IF(RD) 10,11,11
 13    IF (RD) 11,99,10
 99    PRINT 2
 2     FORMAT (16H GAMMA INFINITE     )
 11    CALL BES(1,GAB,0,BESJ1,T)
       CALL BES(0,GAB,0,BESJ0,T)
       E1=BESJ1
       E0 =BESJ0
       BB=RR*GAP*E1/E0
 91    CC=C1*(B0+F*(B1))
       DD= D1* (A0- F*(A1))
```

```
      EE=-CO*(BO+F*(B1))
      FF= DO*(AO-F*(A1))
      XNUM2 = CC+DD
      DEN2 = EE +FF
      Z=XNUM2/  DEN2
      ZY=Z/BB
      ALFA=ABSF(ZY-1.)
      EPS=0.1
      IF (ALFA-EPS) 20,20,59
20    PRINT 5,X,Y,Z,ZY,F,BB
      GO TO 95
10    HAP = -GAP
      FO = BESI(0.C,GAB)
      F1= BESI(1.0,GAB)
93    HCC=C1*(BO+F*(B1))
      HDD= D1*(AO-F*(A1))
      HEE = -CO*(BO+F*(B1))
      HFF= DO*(AO-F*(A1))
      HBB=RR*HAP*F1/FO
      DHN=HEE+HFF
      HNM=HCC+HDD
      HZ=HNM/DHN
      HZY=HZ/HBB
      HLFA= ABSF (HZY-1.0)
      EPS=0.1
      IF(HLFA-EPS)21,21,59
59    IF(SENSE SWITCH 2) 105,60
105   IF(SENSE SWITCH 3)106,107
106   A=A+.000005
      GO TO 102
107   A=A-.000005
      GO TO 102
 60   CONTINUE
21    PRINT 15,X,Y,HZ,HZY,F,HBB
      PRINT 16
95    KK=K-4
      X1(KK)=X
      Y1(KK)=Y
      NUMPTS=KK
50     CONTINUE

101   PRINT 5,X,Y,Z,ZY,F,BB
      PRINT 5,HZ,HZY,F,HBB,Q,RD
      CALL GRAPH (NUMPTS,X1,Y1,8)
      IF(SENSE SWITCH 3) 128,41
128   II=100
      LL=M+II
      GO TO 43
41    CONTINUE
40    CONTINUE
      STOP
      END
      SUBROUTINE BESS (NO,X,KODE,RESULT,T)
      DIMENSION T(1000)
      PI=3.1415926536
      IF (KODE) 41,1,2
    1 CALL BES (NO,X,0,RESULT,T)
      RETURN
    2 IF (KODE-1) 41,3,4
    3 CALL BES (NO,X,1,RESULT,T)
      RETURN
    4 IF (KODE-2) 41,5,6
    5 IF(NO-1)  11,11,12
   12 PRINT 13
   13 FORMAT (34H1ORDER ERROR FOR K AND Y FUNCTIONS)
   14 STOP 14
   11 IF(X-1.) 15,15,16
   16 T(1)=1./X
      DO 240 I=2,12
  240 T(I)=T(I-1)*T(1)
```

```
      IF(NO)  21,20,21
   20 XG0=1.2533141373-.1566641816*T(1)+.0881112782*T(2)-.0913909546*
     1T(3)+.1344596228*T(4)-.2299850328*T(5)+.3792409730*T(6)
     2-.5247277331*T(7)+.5575368367*T(8)-.4262632912*T(9)
     3+.2184518096*T(10)-.0668097672*T(11)+.0091893830*T(12)
      RESULT = EXPF(-1.*X)/SQRTF(X)*XG0
      RETURN
   21 IF (NO-1)  12,22,12
   22 XG1= 1.2533141373 +.4699927013*T(1)-.1468582957*T(2)
     1+.1280426636*T(3)-.1736431637*T(4)+.2847618149*T(5)
     2-.4594342117*T(6)+.6283380681*T(7)-.6632295430*T(8)
     3+.5050238576*T(9)-.2581303765*T(10)+.0788000118*T(11)
     4-.0108241775*T(12)
      RESULT = EXPF(-1.*X)/SQRTF(X)*XG1
      RETURN
   15 CALL BES (1,X,1,XI1,T)
      XI0=T(1)
      T(2)=X*X/4.
      DO 310 I=4,12,2
  310 T(I)=T(I-2)*T(2)
      SUM  = -.57721566     +.42278420 *T(2)  + .23069756 * T(4)
     1       +.03488590*T(6)+.00262698 *T(8)  + .00010750 * T(10)
     2       +.00000740*T(12)
      ANSK0 = SUM - LOGF(X/2.) * XI0
      IF(NO)  31,30,31
   30 RESULT = ANSK0
      RETURN
   31 IF(NO-1)  12,32,12
   32 RESULT = (1./X -ANSK0*XI1)/XI0
      RETURN
    6 IF (KODE-3)  41,40,41
   41 PRINT 42
   42 FORMAT    (11H1KODE ERROR)
   43 STOP 43
   40 IF (NO-1)  50,50,12
   50 T(1)=X/3.
      DO 400 I=2,12
  400 T(I)=T(I-1)*T(1)
      IF (3.-X) 52,51,51
   51 SUMY =   .36746691     + .60559366 * T(2) - .74350384 * T(4)
     1       +.25300117*T(6)- .04261214 * T(8) + .00427916 * T(10)
     2       -.00024846*T(12)
      CALL BES(1,X,0,XJ1,T)
      XJ0=T(1)
      Y0=2./PI*LOGF(X/2.)*XJ0+SUMY
      IF (NO)  53,54,53
   54 RESULT =Y0
      RETURN
   53 IF(NO -1)  12,55,12
   55 RESULT=(XJ1*Y0-2./(PI*X))/XJ0
      RETURN
   52 IF ( 4.-X)  59,60,60
   60 T(1)=X/3.
      DO 402 I=2,12
  402 T(I)=T(I-1)*T(1)
      SUMF0 =.79788456      -.00000077 *3./X    -.00552740/T(2)
     1       -.00009512/T(3)+.00137237 /T(4)     -.00072805/ T(5)
     2       +.00014476/T(6)
      SUMS  =.78539816      +.04166397 *3./X    +.00003954/ T(2)
     1       -.00262573/T(3)+.00054125 /T(4)    +.00029333/ T(5)
     2       -.00013558/T(6)
      Y0 = SUMF0/ SQRTF(X) * SINF (X-SUMS)
      IF (NO)   71,70,71
   70 RESULT =Y0
      RETURN
   71 IF (NO-1) 12,555,12
  555 CALL BES(1,X,0,XJ1,T)
      XJ0=T(1)
      GO TO 55
   59 T(1)=4./X
```

```
      DO 401 I=2,12
  401 T(I)=T(I-1)*T(1)
      IF (NO)  12,73,72
   73 P0 = .3989422793      -.0017530620 *T(2)   +.0001734300 *T(4)
     1    -.0000487613*T(6)+.0000173565 *T(8)   -.0000037043 *T(10)
      Q0 =  -.0124669441      +.0004564324*T(2)   -.0000869791 * T(4)
     1      +.0000342468*T(6)-.0000142078*T(8)   +.0000032312 * T(10)
      Y0 = 2./SQRTF(X)*(P0*SINF(X-PI/4.)+4./X*Q0*COSF(X-PI/4.))
      RESULT=Y0
      RETURN
   72 IF (NO-1)   12,74,12
   74 P1 =     .3989422819    +.0029218256*T(2)    -.0002232030 *T(4)
     1       +.0000580759*T(6)-.0000200920*T(8)   +.0000042414 * T(10)
      Q1 =    .0374008364      -.0006390400*T(2)   +.0001064741 * T(4)
     1       -.0000398708*T(6)+.0000162200*T(8)   -.0000036594 * T(10)
      Y1 = 2./SQRTF(X)*(P1*SINF(X-3.*PI/4.)+4./X*Q1*COSF(X-3.*PI/4.))
      RESULT=Y1
      RETURN
      END
      SUBROUTINE BES(NO,X,KODE,RESULT,T)
      DIMENSION T(100)
      KLAM=1
      KO=NO+1
1009  IF(X) 81,101,82
      ERR=.001
81    IF (X+ERR)108,101,101
82    IF(X-ERR)101,101,108
101   IF(NO)103,102,105
102   T(KO)=1.0
      RESULT = 1.0
      RETURN
103   IF(KO)106,104,105
104   RESULT=9.999999999E200
      RETURN
105   RESULT=0.0
      RETURN
106   PRINT 107
107   FORMAT(55H1NEGATIVE ORDER NOT ACCEPTED IN BESSEL FUNCTION ROUTINE)
1071  STOP 1071
108   IF(NO)106,1081,1081
1081  IF(KODE)11,12,11
11    KLAM=KLAM+1
   12 JO=2*XABSF(XFIXF(X))
      MO=NO
      IF(MO-JO)2,21,21
2     MO=JO
21    MO=MO+11
22    T(MO)=0.
      LUB=MO-1
      T(LUB)=1.0E-300
      GO TO (23,51),KLAM
23    F=2*LUB
231   ENA(-3)RAD(MO)
      LIL2(MO),ENA(T).
      INA(1)SAU(233B)
      INA(1)SAU(233A)
      INA(1)SAL(233A)
232   LDA(F)FSB(2.)
      STA(F)FDV(X)
233A  FMU2(N)FSB2(N)
233B  STA2(N)IJP2(232)
      SUM=T(1)
      GO TO (39,69),KLAM
   39 M3=MO+3
      DO 4 J=3,M3,2
4        SUM=SUM+2.*T(J)
      F=1./SUM
      DO 5 J=1,KO
5        T(J)=T(J)*F
      RESULT=T(KO)
```

```
      RETURN
51    KON=7777777776777777B
      LDA(KON),RAD(233A)
      GO TO 23
69    LAC(KON),RAD(233A)
      M3=MO+3
      DO 7 J=2,M3
7        SUM=SUM+2.*T(J)
      F=1./SUM*EXPF(X)
      DO 8 J=1,KO
8        T(J)=T(J)*F
      RESULT=T(KO)
      END
      SUBROUTINE RGAM (X,Z)
      DIMENSION B(13)
      B(1) = -.422784335092
      B(2) = -.233093736365
      B(3) = .191091101162
      B(4) = -.024552490897
      B(5) = -.017645242118
      B(6) = .008023278113
      B(7) = -.000804541335
      B(8) = -.000360851491
      B(9) = .000145624324
      B(10) = -.000017527917
      B(11) = -.000002625721
      B(12) = .000001328554
      B(13) = -.000000181220
      Z = B(13)
      I = 12
301   Z = Z*X + B(I)
      I = I-1
      IF (I+1) 302,302,301
302   Z = (Z+1.)*X*(X+1.)
      END

      SUBROUTINE RCPGAMR(X,Z)
      IF (X-1.) 208,202,203
202   Z = 1.
      RETURN
203   Y = 1.
205   X = X - 1.
      Y = Y*X
      IF (X-1.) 206,204,205
204   Z = 1./Y
      RETURN
206   CALL RGAM (X,Z)
      Z = Z/Y
      RETURN
208   INT = X
      Q = INT
      IF(X-Q) 211,209,211
209   Z = 0.0
      RETURN
211   IF (X+1.) 212,209,213
213   CALL RGAM(X,Z)
      RETURN
212   Y = X
216   X = X + 1.
      IF (X+1.) 214,209,215
214   Y = Y*X
      GO TO 216
215   CALL RGAM(X,Z)
      Z = Y*Z
      END
      FUNCTION BESI(FN,Z)
      IF(Z) 4,5,5
4     PRINT 6
6     FORMAT( 42H BESI NOT PROGRAMMED FOR NEGATIVE ARGUMENT  )
      PRINT 7
```

```
7     FORMAT( 45H BESI COMPUTED FOR ABSOLUTE VALUE OF ARGUMENT     )
5     Z=ABSF(Z)
      IF(MODF(FN,1.)) 8,9,8
9     FN=ABSF(FN)
8     FK=1.
      FN1=FN+1.
      FN2=FN+2.
      CALL RCPGAMR(FN1,ZA)
      CALL RCPGAMR(FN2,ZB)
      AI=(Z/2.)**2*ZB
      A=ZA+AI
3     FK=FK+1.
      AI=AI*(Z/2.)**2/((FK+FN)*FK)
      FN2=FN2+1.
      A=A+AI
      IF(ABSF(AI)-ABSF(A)*10.**(-14)) 2,3,3
2     BESI=(Z/2.)**FN*A
      END
      FUNCTION BESK(FN,Z)
      FN=ABSF(FN)
      IF(MODF(FN,1.)) 13,12,13
13    FA=-FN
      BESK=1.570796327*(BESI(FA,Z)-BESI(FN,Z))/(SINF(3.141592654*FN))
      RETURN
12    N=FN
      A=(-1.)**(N+1)*BESI(FN,Z)*LOGF(1.781072418*Z/2.)
      HZ=Z/2.
      BIBA=1.
      BIA=0.
      BIB=0.
      IF(N) 100,100,101
100   B=0.
      GO TO 105
101   DO 102 KK=1,N
      FKK=KK
      BIBA=BIBA/FKK
102   BIB=BIB+1./FKK
105   BI=BIBA
      B=BIBA*BIB
      FK=1.
103   FNK=FN+FK
      BIA=BIA+1./FK
      BIB=BIB+1./FNK
      BI=BI*HZ**2/(FK*FNK)
      FK=FK+1.
      TEST=BI*(BIA+BIB)
      B=B+TEST
      IF(ABSF(TEST)-ABSF(B)*10.**(-14)) 104,103,103
104   B=(-HZ)**N*B
      IF(N-1) 200,201,202
200   C=0.
      GO TO 300
201   C=1.
      GO TO 204
202   NA=N-1
      NN=1
      DO 203 J=1,NA
203   NN=NN*J
      C=NN
      CB=C
205   KD=1
      FKD=KD
      CB=(-1.)**KD*CB*HZ**2/((FN-FKD)*FKD)
      KD=KD+1
      C=C+CB
      IF(KD-N) 205,204,205
204   C=C*HZ**(-N)
300   BESK=A+(B+C)/2.
      END
      END
```

```
0                                                          10     9                    2
02 OMEGA BETA PLOT,C1=3.,C2=0.5 C3=2.0
02 COLIN M. JONES
0
0                                                          10     9                    2
02 OMEGA BETA PLOT,C1=3.,C2=0.5 C3=2.0
02 COLIN M. JONES
0
0                                                          10     9                    2
02 OMEGA BETA PLOT,C1=3.,C2=0.5 C3=2.0
02 COLIN M. JONES
0
0                                                          10     9                    2
02 OMEGA BETA PLOT,C1=3.,C2=0.5 C3=2.0
02 COLIN M. JONES
0
0                                                          10     9                    2
02 OMEGA BETA PLOT,C1=3.,C2=0.5 C3=2.0
02 COLIN M. JONES
0
0                                                          10     9                    2
02 OMEGA BETA PLOT,C1=3.,C2=0.5 C3=2.0
02 COLIN M. JONES
0
0                                                          10     9                    2
02 OMEGA BETA PLOT,C1=3.,C2=0.5 C3=2.0
02 COLIN M. JONES
0
0                                                          10     9                    2
02 OMEGA BETA PLOT,C1=3.,C2=0.5 C3=2.0
02 COLIN M. JONES
0
0                                                          10     9                    2
02 OMEGA BETA PLOT,C1=3.,C2=0.5 C3=2.0
02 COLIN M. JONES
0
0                                                          10     9                    2
02 OMEGA BETA PLOT,C1=3.,C2=0.5 C3=2.0
02 COLIN M. JONES
0
0                                                          10     9                    2
02 OMEGA BETA PLOT,C1=3.,C2=0.5 C3=2.0
02 COLIN M. JONES
0
0                                                          10     9                    2
02 OMEGA BETA PLOT,C1=3.,C2=0.5 C3=2.0
02 COLIN M. JONES
0
0                                                          10     9                    2
02 OMEGA BETA PLOT,C1=3.,C2=0.5 C3=2.0
02 COLIN M. JONES
0
0                                                          10     9                    2
02 OMEGA BETA PLOT,C1=3.,C2=0.5 C3=2.0
02 COLIN M. JONES
0
0                                                          10     9                    2
02 OMEGA BETA PLOT,C1=3.,C2=0.5 C3=2.0
02 COLIN M. JONES
0
0                                                          10     9                    2
02 OMEGA BETA PLOT,C1=3.,C2=0.5 C3=2.0
02 COLIN M. JONES
0
0                                                          10     9                    2
02 OMEGA BETA PLOT,C1=3.,C2=0.5 C3=2.0
02 COLIN M. JONES
0
0                                                          10     9                    2
```